East African Journal of Engineering
eaje.eanso.org
Volume 7, Issue 1, 2024
Print ISSN: 2707-5389 | Online ISSN: 2707-5397
Title DOI: https://doi.org/10.37284/2707-5397

EAST AFRICAN NATURE & SCIENCE ORGANIZATION

Original Article

Distribution of Floods Frequency of Manafwa River, Uganda

Joseph Micheal Okoth[1], Dr. Daniel Otim, PhD[1] & Dr. Edwin Kamalha, PhD[1]*

[1] Busitema University, P. O. Box 236, Tororo, Uganda.
* Author for Correspondence ORCID ID: https://orcid.org/0009-0002-0262-3108; Email: okothrujema@gmail.com

Article DOI : https://doi.org/10.37284/eaje.7.1.1670

Publication Date:

24 January 2024

Keywords:

Flood Frequency, River Flows, Manafwa River, Floodplains, Distribution Analysis

ABSTRACT

The objective of this study was to analyse Manafwa River flood frequency in Eastern Uganda. Analysis of Manafwa River maximum annual flows from 1949-2015 was undertaken using Log Pearson 3 distribution in comparison with Gumbel, Normal and Log Normal distributions to determine frequency of occurrence and magnitude of extreme floods. Statistical analysis including goodness of fit tests of chi-square, Kolmogorov-Smirnov and Anderson-Darling tests were used to generate the most suitable probability distribution model. The results show quantile magnitudes lowest for Log Normal distribution at 43.59 m3/s and highest for Log Pearson 3 distribution at 51.67 m3/s. The 5-year quantile estimates are highest for Normal and Log Pearson at 70.37 m3/s and 63.99 m3/s respectively. The 10-year quantile estimates are highest for Log Normal and lowest for Log Pearson 3 distributions at 87.57 m3/s and 75.13 m3/s respectively. The 100-year quantile estimates are lowest for Normal and highest for Log Normal distributions at 108.57 m3/s and 154.66 m3/s respectively. The 200-year quantile estimates are lowest for Normal and highest for Log Normal distributions respectively at 114.980 m3/s and 177.16 m3/s respectively. Log Pearson 3 distribution emerged as best fit for data. From the statistical analysis, LP 3 probability distribution presents the most accurate regression coefficient at 0.8486 and the most suitable distribution of goodness of best fit using A-D, K-S and Chi square tests followed by the Gumbel distribution. The tests yield 0.15666, 0.04855 and 0.88502 for A-D, K-S and Chi square tests respectively for the LP 3 distribution. There is an increasing upward trend of the discharges at Manafwa River floodplains at higher probabilities of exceedance across all the probability distributions due to varrying climatic changes and rapid landuse changes in the Manafwa catchment. Manafwa river floodplains have the capacity to accommodate and boost crop production and productivity. Any nutrients lost to leaching could be gained from subsequent fallowing and sustainable soil fertility management including; proper drainage, crop rotation, adding organic manure, cover cropping and among others.

APA CITATION

Okoth, J. M., Otim, D. & Kamalha, E. (2024). Distribution of Floods Frequency of Manafwa River, Uganda *East African Journal of Engineering*, 7(1), 1-20. https://doi.org/10.37284/eaje.7.1.1670

CHICAGO CITATION

Okoth, Joseph Micheal, Daniel Otim and Edwin Kamalha. 2024. "Distribution of Floods Frequency of Manafwa River, Uganda". *East African Journal of Engineering* 7 (1), 1-20. https://doi.org/10.37284/eaje.7.1.1670.

Article DOI: https://doi.org/10.37284/eaje.7.1.1670

HARVARD CITATION

Okoth, J. M., Otim, D. & Kamalha, E. (2024) "Distribution of Floods Frequency of Manafwa River, Uganda", *East African Journal of Engineering*, 7(1), pp. 1-20. doi: 10.37284/eaje.7.1.1670.

IEEE CITATION

J. M., Okoth, D., Otim & E., Kamalha "Distribution of Floods Frequency of Manafwa River, Uganda" *EAJE*, vol. 7, no. 1, pp 1-20, Jan. 2024.

MLA CITATION

Okoth, Joseph Micheal, Daniel Otim & Edwin Kamalha. "Distribution of Floods Frequency of Manafwa River, Uganda." *East African Journal of Engineering*, Vol. 7, no. 1, Jan. 2023, pp. 1-20, doi:10.37284/eaje.7.1.1670.

INTRODUCTION

A flood is a big amount of water generated from a particular source such as; river, pond, snow melting glaciers, broken dam, pipe towards a previously dried and unsubmerged area (Njoku & Okoro, 2015). Globally, flooding is arguably the commonest and most damaging natural disaster (Malik & Pal, 2021). Lately, river Nyamwamba in Uganda has experienced pronounced flood events partly due to the El-Nino rains that led to rivers overflowing and bursting their banks, into the neighbourhood (Mayega et al., 2015).

The Manafwa catchment covers an area of 2280 km^2 and is composed of both mountainous and low land areas (Cecinati, 2013). The catchment lies between 4300 m above sea level at the Elgon ranges and 1000 m above sea level in the Butaleja lowlands (Bingwa, 2013). It is composed of numerous gauged rivers originating from the Elgon ranges; Ngenge, Namatala, Malaba/Lwakhakha, Manafwa, Simu, Sironko, Muyembe and Sipi rivers.

Land use changes associated with development affect flooding by clearing vegetation leaving the soil surface bare (Ogbodo, 2011). Although the increase of flood events in Manafwa catchment are usually attributed to climate change, the nexus between land use and increased surface water run-off suggests that land use changes especially farming and settlements may also impact floods on the same catchments (Bingwa, 2013). A study by Cecinati (2013) shows that although regular rainfall amounts in Manafwa catchment rainy season has reduced lately, her flood frequency and magnitude have increased because of increasing intensity of reducing frequent intensive rainfall events on drier soil surfaces and the land use changes.

Floods downstream of Manafwa catchment are usually caused by the extreme but less frequent rainfall in the Bududa area. Bududa located upstream of Manafwa River and at the foot of Mount Elgon is more affected by landslides than it is by floods (Obubu et al., 2021). During the 2010 deadly disaster, about 388 people lost their lives in Bududa due to landslides and over 38,780 were affected by floods in Butaleja (Agrawal et al., 2013). Butaleja is located downstream of the Manafwa catchment and therefore, most flooded often (Obubu et al., 2021). Although Butaleja is mostly fertile due to reception of dumped top soils and crop nutrients from the upstream, this leaves prime Butaleja agricultural land and crops more susceptible to flooding (Châu, 2014).

Flood Frequency Analysis

Flood frequency analysis is the dimensionless mechanism used to relate the magnitude of extreme events to their frequency of occurrence (return period) through the use of probability distributions based on past recorded peak discharge data at various gauge stations along a river (Bai et al., 2019). One of the most commonly used assumptions in flood frequency analysis is that annual maximum flood peaks are independently and identically distributed, extracted and conform to the theoretical frequency distribution (Franks & Kuczera, 2002). However, persistent climate modes, such as El Nino-Southern Oscillation (ENSO), modulate regional climates on annual/inter-annual timescales globally. Such persistence raises questions whether annual maximum floods are indeed independently and identically distributed. A study

Article DOI: https://doi.org/10.37284/eaje.7.1.1670

by Franks and Kuczera (2002) revealed that the assumption that annual maximum floods are identically and independently distributed is inconsistent with the gauged flood evidence from 41 sites in New South Wales, Australia.

Determination of magnitude of design floods with a specified exceedance probability is required for design and management of hydraulic structures (bridges, dams) and flood risk management projects. Besides using past flow records to direct projected performance of future flood occurrences, frequency analysis also deploys hydrologic models to generate data to illustrate the estimation of exceedance probability and return periods (Kundu et al., 2014). The longer the period of observed flood peak series, the more realistic the results of the flood frequency analysis because the parameters of the probability distribution functions estimated from longer sample series tend to be close to their population values (Wan Deraman et al., 2017). This study aimed to assess flood frequency analysis of River Manafwa.

MATERIALS AND METHODS

Study Area

The study was carried out at Butaleja floodplains on the Butaleja-Kachonga bridge crossing at coordinate of (0.92829, 33.990378). Manafwa River starts from coordinates of (1.089092, 34.46106) and ends at coordinates of (0.943084, 33.98428).

Figure 1: A map showing the Manafwa catchment area

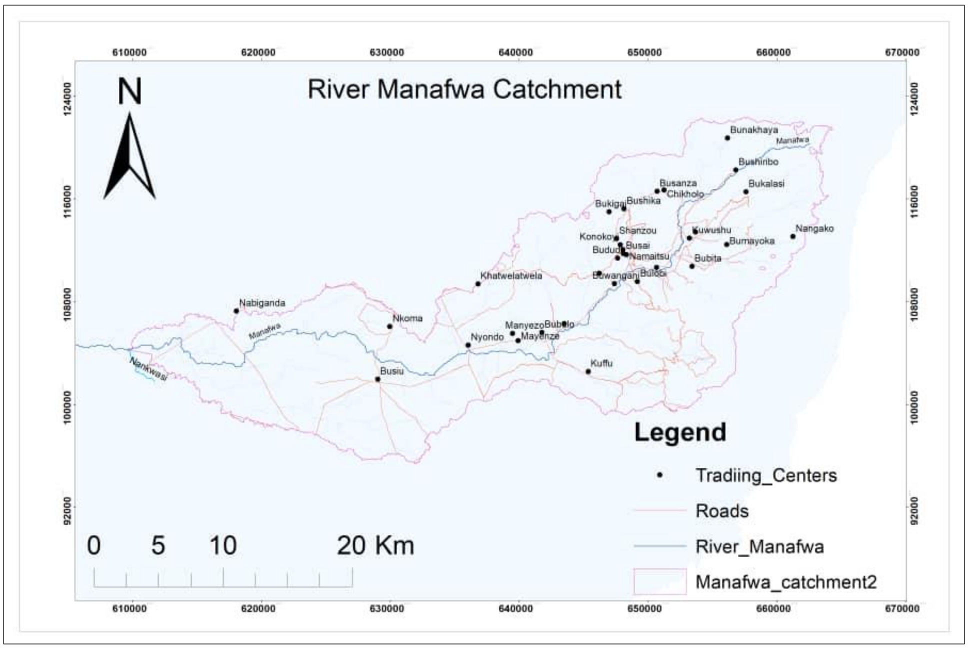

Source: (ArchGIS, 2022)

Manafwa catchment just like other parts of Uganda experiences two distinct rainy seasons (bimodal) a year crossing equator; from north to south and from south to north. The first wet season is usually March - May (MAM) with its peak in April, receives 538 mm of rainfall whereas the second one in September - November (SON) with peaks in October 418 mm of rainfall (UNMA). Interestingly, both MAM and SON wet seasons coincide with passage of Inter Tropical Convergence Zone (ITCZ) that lags behind the overhead sun by about a month while two dry spells separate wet seasons from June to August and December to February (Ogwang et al., 2012). The MAM rainy season is usually more intense (Cecinati, 2013).

River Data

The secondary data used was daily river flow data from 1949 to 2015 obtained from measurements by Ministry of Water and Environment (MWE)'s Directorate of Water Resources Management

Article DOI: https://doi.org/10.37284/eaje.7.1.1670

(DWRM). Although Manafwa River catchment recording started a year earlier in 1948, both river Malaba and Namatala had missing data in 1948 just like River Manafwa.

This was reason for using daily river flows from the year 1949. Similarly, the years after 2015 had numerous missing data and were still under compilation and arrangement.

Flood Frequency Analysis Probability Distributions

Probabilistic model relies on use of existing data to forecast future scenario while deterministic model rely on the different physical parameters to bring out result and verify it with existing data to develop a best fit model (Kundu et al., 2014).

Although many probability distributions exist, the Log-Pearson Type III (LP 3) and Extreme Values (EV I) are the most commonly used because they provide the best fits. For lower return periods below 25 years, Extreme Values and Log-Pearson Type III may be utilized for flood frequency analysis while Log-Normal distribution gives higher quantile magnitudes higher degree of reliability (Malik & Pal, 2021).

Gumbel Distribution

From Thomopoulos et al. (2018), equations 1 to 10 explain various functions of the Gumbel distribution;

I. Probability Density Function (PDF)

$$f(x) = \frac{1}{\alpha}\exp\left[-\frac{x-u}{\alpha} - \exp\left[-\frac{x-u}{\alpha}\right]\right] \quad (1)$$

Where: f(x) = probability density function, x = random variables, u = Mode of distribution, α = probability factors

II. Cumulative Distribution Function (CDF)

$$F(x) = \exp\left[-\exp\left[-\frac{x-u}{\alpha}\right]\right] \quad (2)$$

Where: F(x) = Cummulative Distribution Function

III. Factor

$$\alpha = \frac{\sqrt{6\sigma}}{\pi} \quad (3)$$

Where: σ is the standard deviation

IV. Mode of the Distribution

$$u = \mu - 0.5772\alpha \quad (4)$$

Where: μ = mean

V. Reduced y-variate, y

$$y = \frac{x-u}{\alpha} \quad (5)$$

VI. Probability of exceedance

$$F_1(X) = 1 - F(X) = \frac{1}{T} \quad (6)$$

Where T is Return period in years

VII. Return period, T

$$T = \frac{n+1}{m} \quad (7)$$

Where n is the number of years of record, m is the rank got after re-arranging the annual maximum river flow series in descending order of magnitude with the maximum being assigned the rank of 1.

VIII. Y-variate of return period, T

$$y_T = -\ln T\left[\ln\frac{T}{T-1}\right] \quad (8)$$

Where y_T is the y-variate of return period T

IX. Extreme Event Magnitude at return period, T for Gumbel distribution

$$X_T = \bar{x} + K_T s \quad (9)$$

Where K_T- frequency factor, s- standard deviation

X. Frequency Factor

Article DOI: https://doi.org/10.37284/eaje.7.1.1670

$$K_T = -(\frac{\sqrt{6}}{\pi}) + \left\{0.5772 + \ln\left[\ln\left(\frac{T}{T-1}\right)\right]\right\} \quad (10)$$

Normal distribution

From Pamuttu et al. (2018), Equation 11 to Equation 15 represent normal distribution;

i. Probability Distribution Function;

$$f_x(x) = \frac{1}{\sigma\sqrt{2\pi}} e^{-\frac{1}{2}(\frac{x-\mu}{\sigma})^2} \quad (11)$$

ii. Mean of the Distribution

$$\mu = \frac{1}{n}\sum_{i=1}^{n} X_i \quad (12)$$

Where: X_i = the magnitude of the *i*th event, n = the number of events

iii. Standard Deviation of the Distribution

$$\sigma = \left[\frac{\sum_{i=1}^{n}(x-\mu)^2}{n-1}\right]^{\frac{1}{2}} \quad (13)$$

iv. Extreme Event Magnitude, X_T at return period, T for Normal distribution

$$X_T = \mu + K\sigma \quad (14)$$

v. Frequency factor for Normal and Log Normal distributions

$$K_T = \frac{X_T - \mu}{\sigma} \quad (15)$$

Log-Normal Distribution

From Alghazali & Alawadi (2014), we obtain Equation 16 to Equation 18 for

Log-Normal distribution;

i. Probability distribution function

$$f(x) = \frac{1}{x\sigma\sqrt{2\pi}} \exp\left[-\frac{(y-\mu_y)^2}{2\sigma^2{}_y}\right]$$; for x > 0, y = log x

ii. Mean value for y = log x

$$\mu_y = \frac{1}{n}\sum_{i=1}^{n} y \quad (16)$$

iii. Standard deviation for y = log X

$$\sigma_y = \frac{\sum_{i=1}^{n}(y-\mu_y)}{n-1} \quad (17)$$

iv. Extreme value event

$$Y_T = \mu_y + K_T\alpha_y \quad (18)$$

Log Pearson III distribution

LP3 is a member of the family of Pearson type distributions and is also referred to as the three-parameter distribution because it uses the shape, scale and location parameters/lower or upper bound (Farooq et al., 2018). According to Kamal et al. (2017a), Log Pearson III (LP3) distribution method is known for maintaining data originality and giving a better fit over other probability distributions for longer return periods. The LP3 is currently the preferred and standard probability distribution model used by the U.S. and Australia because of its appropriate capacity to estimate extreme flood events (Dis et al., 2018). The distribution has been found to be yielding good results in many applications, particularly for flood peak data (Bhat et al., 2019). It is also capable of fitting frequency relations that are highly skewed due to hydrologic reasons (Malik & Pal, 2021; Roy et al., 2015). According to Ehiorobo and Uso, (2014), the procedure for the determination of Log Pearson 3 distribution discharges are as follows;

i. The annual flood series (Q) were assembled and ranked.

ii. The mean μ_y, the standard deviation, σ_y and skew coefficient (G) of the data are

Article DOI: https://doi.org/10.37284/eaje.7.1.1670

calculated using equations 19, 20, 21 and 22 respectively (Dis et al., 2018).

a) Mean value for y = log x

$$\mu_y = \frac{1}{n}\sum_{i=1}^{n} y \quad (19)$$

b) Standard deviation for y = log X

$$\sigma_y = \frac{\sum_{i=1}^{n}(y-\mu_y)}{n-1} \quad (20)$$

The skewness, G is an important hydrological characteristic which gives a measure of shape of a sampling distribution (Kundu et al., 2014).

c) Skewness, G

$$G = \frac{n\sum(y-\mu_y)^3}{(n-1)(n-2)(\sigma_y)^3} \quad (21)$$

Where: n = length of data, y-log x, μ_y = mean, K_T - Pearson frequency factor, σ_y = standard deviation of log x.

The log-Pearson Type III distribution uses log transformation of the data from natural to logarithmic units as a base method for flood flow frequency studies (Ibrahim et al., 2016). For Y series, for any recurrence interval, T from Equation 19 gives,

d) Extreme value event of Log Pearson III distribution

$$Y_T = \mu_y + K_T\alpha_y \quad (22)$$

Where: Y_T = log X (logarithm of the discharge of the desired quantile), μ_y = mean, K_T = Pearson frequency factor obtained from standard tables, σ_y = standard deviation of log x

The Goodness of Fit Test

The goodness of fit (GoF) test is a comparison stage for the degree of fit between observed and statistical model and ought to be conducted prior to modeling or any decision-making processes.

Chi Squared Test

According to Farooq et al. (2018), the Chi square goodness of fit test is described by equations 23 to 31;

i. The sample relative frequency factor, f_s is

$$f_s(x_i) = \frac{n_i}{n} \quad (23)$$

Where n_i is the number of observations in i-intervals, and n is total number of observations.

ii. The cumulative frequency, F_s is

$$F_s(x_i) = \sum_{j=1}^{i} f_s(x_i) \quad (24)$$

iii. The incremental probability function $p(x_i)$ is

$$p(x_i) = F(x_i) - F(x_{i-1}) \quad (25)$$

Where F(x) is the probability distribution and f(x) is the probability density functions

iv. The Chi-squared test statistic for goodness of fit is

$$\chi^2 = \sum_{i=1}^{m} \frac{n(f_s(x_i) - p(x_i))^2}{p(x_i)} \quad (26)$$

Where: m = number of intervals / classes, $n(f_s(x_i)$ = Observed frequencies in interval i and $p(x_i)$ is Expected frequencies in interval i

v. Degree of freedom of goodness of fit test

$$v = m - p - 1 \quad (27)$$

Where v is the degree of freedom, m is the number of intervals, p is the number of parameters used in fitting the distribution. The significance level, α = 0.05.

According to Chow et al. (1988), null hypothesis for this test is that the proposed probability distribution adequately fits the data, i.e. calculated χ^2 ought to be less than the tabular χ^2 at α = 0.05

Article DOI: https://doi.org/10.37284/eaje.7.1.1670

significance level or else the hypothesis is rejected.

vi. Standard normal variable, z

$$z = \frac{x-\mu}{\sigma} \tag{28}$$

Kolmogorov-Smirnov (K-S) Test

The Kolmogorov−Smirnov (K−S) test is an alternative non-parametric test that uses cumulative distribution to determine the specific distribution of the data (Aslam, 2019). According to Farooq et al. (2018), the Kolmogorov-Smirnov (K-S) test for goodness of fit test is;

$$D_n = Maximum\left[F_n(X) - F_s(X)\right] \tag{29}$$

Where: F_s = Sample cumulative distribution function, F_n (X) = Cumulative normal distribution function,

For n>40, K-S critical values are calculated as;

$$D_{critical} = \frac{1.36}{n} \tag{30}$$

Therefore, a comparison is made between D_n and $D_{critical}$ (critical K-S test values). If $D_n < D_{critical}$, accept hypothesis, accept hypothesis, is no significant relationship exists between the variables.

Anderson-Darling (A-D) test

The Anderson – Darling test compares expected cumulative distribution function to observed cumulative distribution function (Mehmood et al., 2019). The A-D test statistic (A^2) is:

$$A^2 = -n - \sum_{k=1}^{n} \frac{2k-1}{n} \{\ln Q_k) + \ln\{1 - F(Q_{n+1-k})\}\} \tag{31}$$

Where n – sample size, $Q_1 \ldots Q_n$ is observed data and F is the cumulative distribution function. If A^2 is greater than the critical value of 5018, null hypothesis is rejected (Mehmood et al., 2019).

Article DOI: https://doi.org/10.37284/eaje.7.1.1670

Table 1: Flood analysis computation table

Year	Max flows	Ranked Flow	T, yrs	Probability	Y= log X	y-variate	Year	Max flows	Ranked Flow	T, yrs	Probability	Y= log X	y-variate
1949	39.9	127.3	68	0.01	0.105	4.21	1983	36.2	41.8	2	0.51	1.621	0.32
1950	61.0	100.9	34	0.03	0.012	3.51	1984	17.0	41.3	2	0.53	1.616	0.28
1951	88.1	100.7	23	0.04	0.003	3.10	1985	13.4	41.1	2	0.54	1.614	0.24
1952	45.7	93.6	17	0.06	1.971	0.80	1986	7.3	40.0	2	0.56	1.602	0.20
1953	17.4	90.2	14	0.07	1.965	0.57	1987	24.9	39.9	2	0.57	1.601	0.16
1954	17.4	88.8	11	0.09	1.948	0.38	1988	41.1	38.6	2	0.59	1.587	0.12
1955	46.7	88.3	10	0.10	1.946	0.22	1989	93.6	38.3	2	0.60	1.583	0.08
1956	37.4	88.1	9	0.12	1.945	0.08	1990	109	38.1	2	0.62	1.581	0.04
1957	71.6	86.1	8	0.13	1.935	1.95	1991	58.7	37.4	2	0.63	1.572	0.00
1958	48.2	77.5	7	0.15	1.889	1.84	1992	38.6	36.4	2	0.65	1.561	-0.04
1959	33.4	76.5	6	0.16	1.884	1.73	1993	60.2	36.2	2	0.66	1.559	-0.08
1960	35.3	74.1	6	0.18	1.870	1.64	1994	10.5	35.3	1	0.68	1.548	-0.12
1961	67.4	71.6	5	0.19	1.855	1.55	1995	23.5	34.5	1	0.69	1.537	-0.16
1962	43.9	70.4	5	0.21	1.848	1.47	1996	50.7	33.4	1	0.71	1.524	-0.20
1963	74.1	70.1	5	0.22	1.846	1.39	1997	76.5	39	1	0.72	1.517	-0.24
1964	90.2	67.4	4	0.24	1.829	1.32	1998	60.7	31	1	0.74	1.507	-0.28
1965	34.5	60.7	4	0.25	1.798	1.25	1999	38.3	29.7	1	0.75	1.472	-0.33
1966	41.8	61.4	4	0.26	1.788	1.18	2000	25.7	28.9	1	0.76	1.461	-0.37
1967	88.8	61.0	4	0.28	1.785	1.12	2001	28.9	26.5	1	0.78	1.424	-0.41
1968	77.5	60.2	3	0.29	1.780	1.05	2002	55.0	25.7	1	0.79	1.410	-0.46
1969	30.9	60.2	3	0.31	1.779	1.00	2003	40.2	24.9	1	0.81	1.396	-0.50
1970	88.3	58.7	3	0.32	1.768	0.94	2004	30.1	24.0	1	0.82	1.380	-0.55
1971	24.0	57.1	3	0.34	1.757	0.88	2005	47.9	23.9	1	0.84	1.379	-0.60
1972	70.4	55.0	3	0.35	1.740	0.83	2006	127.3	23.5	1	0.85	1.371	-0.65
1973	36.4	53.4	3	0.37	1.728	0.78	2007	86.1	20.5	1	0.87	1.312	-0.70
1974	60.2	50.2	3	0.38	1.718	0.73	2008	57.1	17.4	1	0.88	1.240	-0.76
1975	50.2	50.7	3	0.40	1.705	0.68	2009	50.2	17.4	1	0.90	1.240	-0.82
1976	41.3	50.2	2	0.41	1.701	0.63	2010	100.7	17.0	1	0.91	1.231	-0.89
1977	61.4	48.2	2	0.43	1.683	0.59	2011	40.0	13.4	1	0.93	1.126	-0.96
1978	53.4	47.9	2	0.44	1.681	0.54	2012	26.5	10.5	1	0.94	1.096	-1.04
1979	70.1	46.7	2	0.46	1.669	0.50	2013	20.5	10.8	1	0.96	1.033	-1.14
1980	10.8	45.7	2	0.47	1.660	0.45	2014	38.1	10.8	1	0.97	1.033	-1.26
1981	10.8	43.9	2	0.49	1.643	0.41	2015	23.9	7.3	1	0.99	0.860	-1.44
1982	29.7	42.0	2	0.50	1.624	0.37							

Article DOI: https://doi.org/10.37284/eaje.7.1.1670

RESULTS AND DISCUSSION

From *Table 1*, n = 67

From Equation 21, mean, μ = 49

From Equation 13, standard deviation, σ = 26

Figure 2: Histogram for annual maximum flow

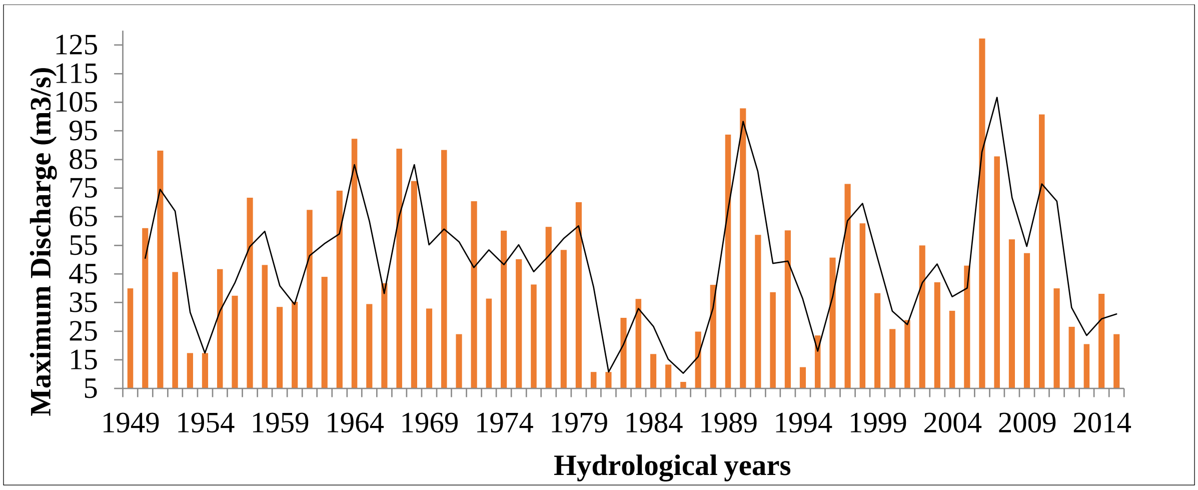

From Figure 2, river Malaba flow data follows Gumbel or Generalised Extreme Value 1

Gumbel Distribution

From Equation 3; Factor, $\alpha = 4$

From Equation 4; Mode of the distribution; $u = 46$

Table 2: Flow magnitude estimates for selected return periods

Return period, T years	Reduced variate, Y_T	Frequency factor, K_T	Discharge magnitude, X_T, m^3/s
2	0.367	-0.160	44.599
5	1.500	0.723	67.332
10	0.250	1.308	80.383
25	3.199	0.048	101.400
50	3.902	0.596	115.508
100	4.600	3.141	129.511
200	5.296	3.683	143.464

Figure 3: Gumbel distribution extreme discharges vs. probability

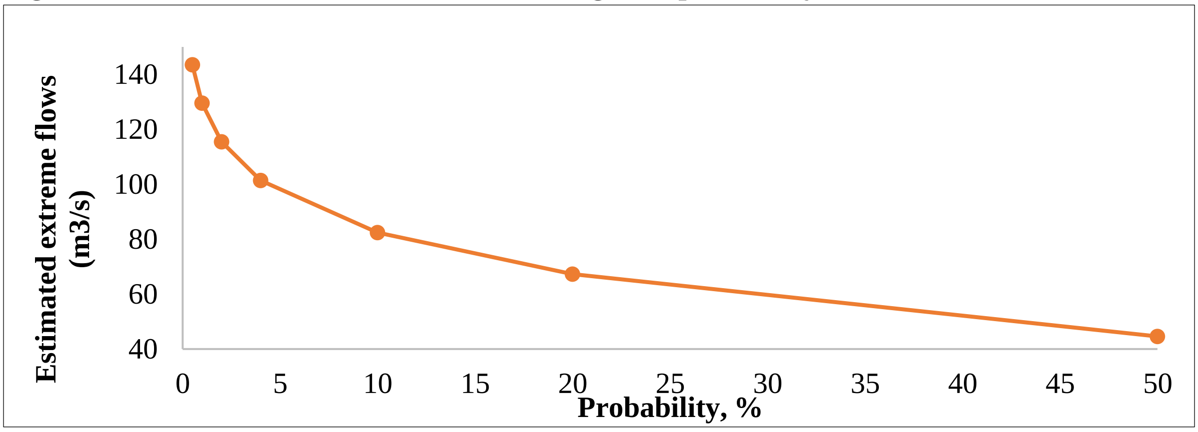

Normal Distribution

From Equation 14 and Equation 15, K_T and X_T are estimated as per *Table 3*.

.

Article DOI: https://doi.org/10.37284/eaje.7.1.1670

Table 3: Normal distribution Flow magnitude estimates for selected return periods

Return period, T	Probability, p	Frequency factor, K_T or Z_T	Discharge magnitude, X_T m^3/s
2	0.5	0.00	48.724
5	0.2	0.84	70.374
10	0.1	1.28	81.690
25	0.04	1.75	93.758
50	0.02	0.05	101.554
100	0.01	0.33	108.566
200	0.005	0.58	114.984

Figure 4: Normal distribution extreme flows vs. probability

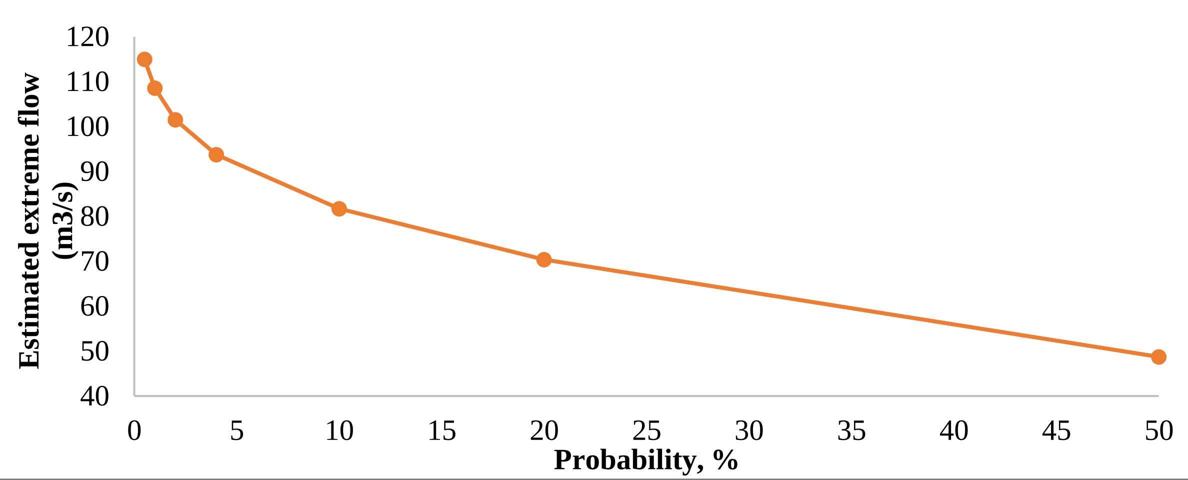

Log-Normal Distribution

$$\mu_y = 1.64, \sigma_y = 0.236$$

From Equation 16 and Equation 17,

Table 4: Computed discharges for Log-Normal distribution

T, years	Frequency factor, K_T	Y_T	X_T (10^Y), (m^3/s)
2	0.00	1.64	43.59
5	0.84	1.84	68.92
10	1.28	1.94	87.57
25	1.75	0.05	113.05
50	0.05	0.12	133.33
100	0.33	0.19	154.66
200	0.58	0.25	177.16

Figure 5: Log Normal distribution extreme discharges vs probability

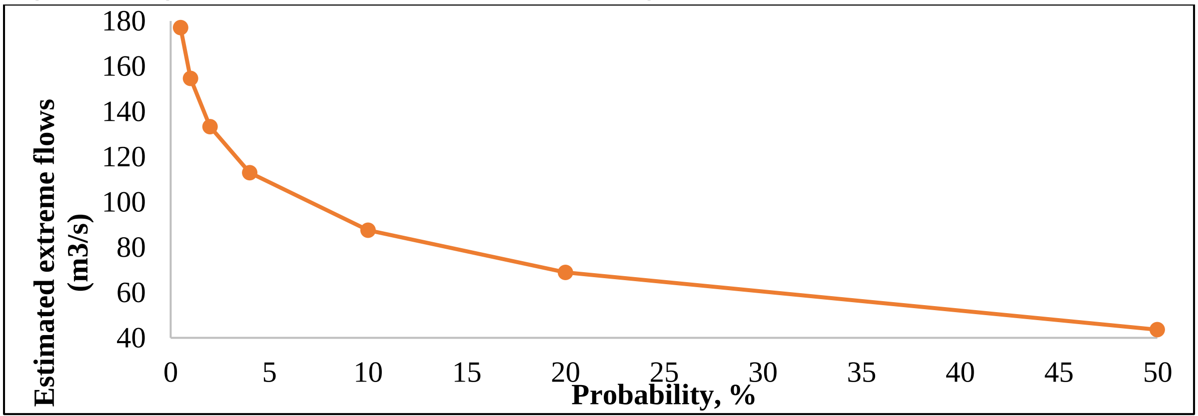

Article DOI: https://doi.org/10.37284/eaje.7.1.1670

Log Pearson III Distribution

From Equation 21, skewness, $G = -0.444$

Table 5: Computed discharges for selected return periods

T, years	Frequency factor, K_T	log X	X_T (m^3/s)
2	0.31	1.71	51.67
5	0.71	1.81	63.99
10	1.00	1.88	75.13
25	1.39	1.97	971
50	1.68	0.04	108.54
100	1.96	0.10	126.93
200	0.25	0.17	148.29

Figure 6: Log Pearson 3 distribution discharges vs. probability

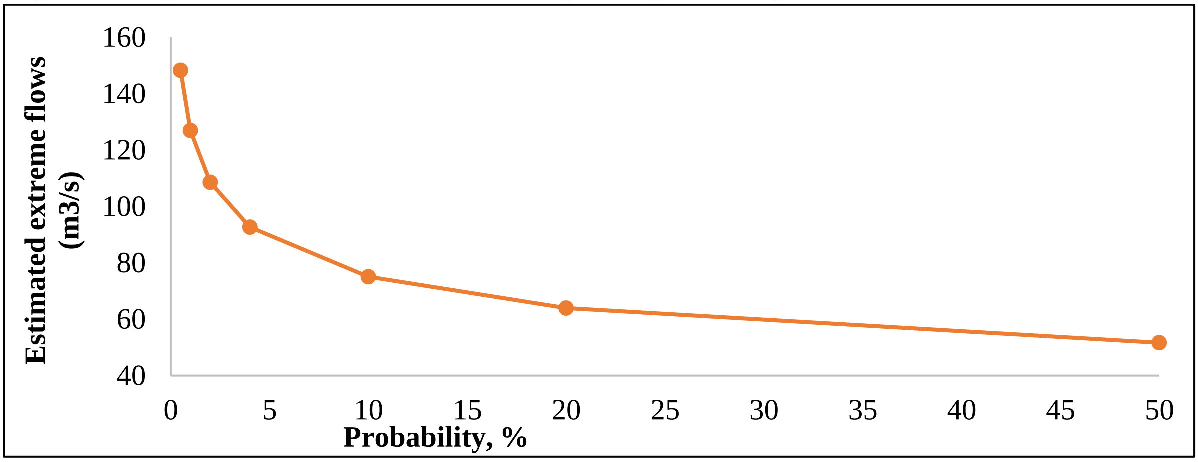

Table 6: Summary of quantile estimates (m3/s) from different probability distributions

Return period	Gumbel	Normal	Log Normal	Log Pearson III
T, years	X_T	X_T	X_T	X_T
2	44.60	48.72	43.59	51.67
5	67.33	70.37	68.92	63.99
10	80.38	81.69	87.57	75.13
25	101.40	93.76	113.05	90.71
50	115.51	101.55	133.33	108.54
100	129.51	108.57	154.66	126.93
200	143.46	114.98	177.16	148.29

Figure 7: Graph summarizing quantile estimates for various Probability Distributions

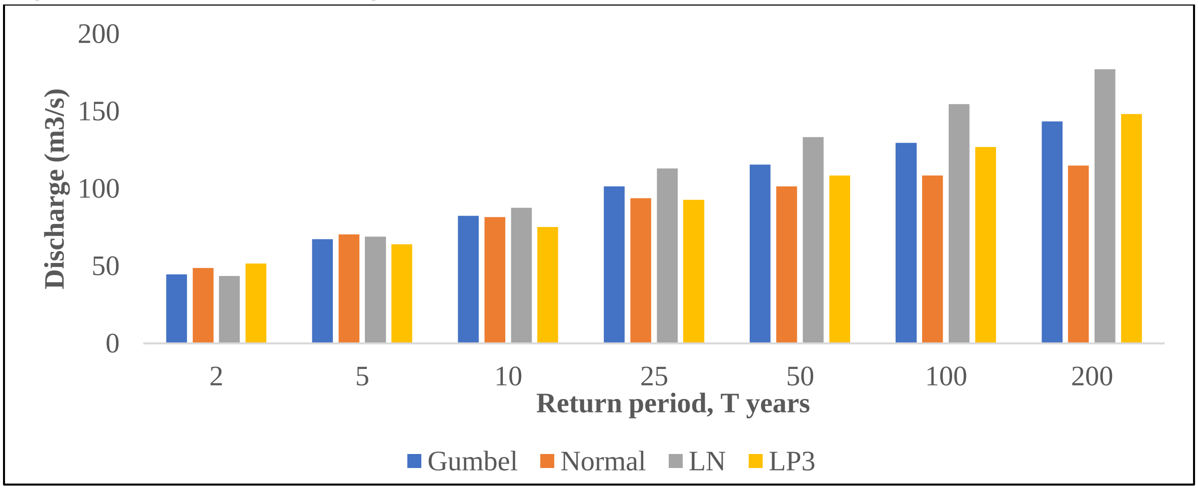

Article DOI: https://doi.org/10.37284/eaje.7.1.1670

Figure 8: CDF for Log Pearson distribution

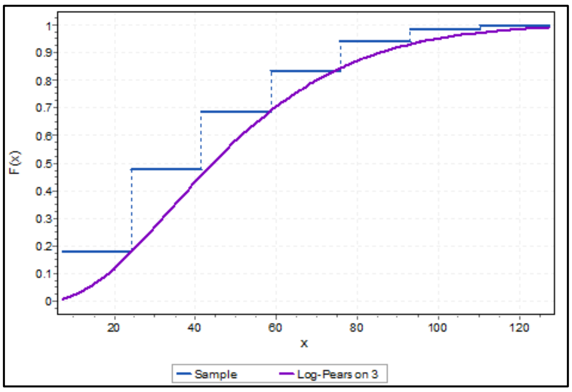

Figure 9: CDF for Gumbel/GEV1 distribution

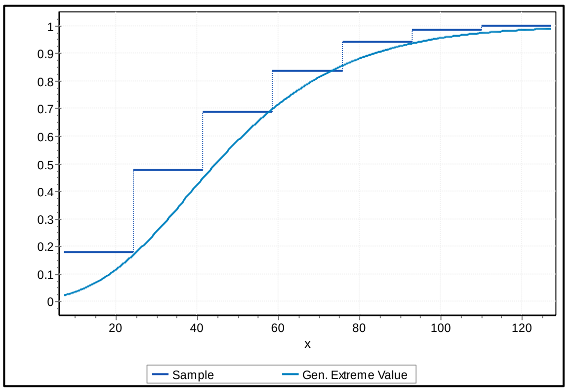

Figure 10: CDF for Lognormal distribution

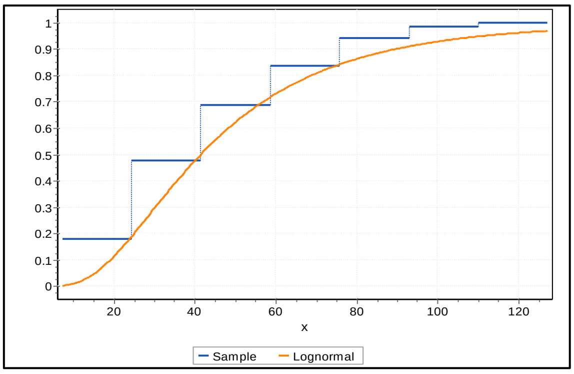

Figure 11: CDF for normal distribution

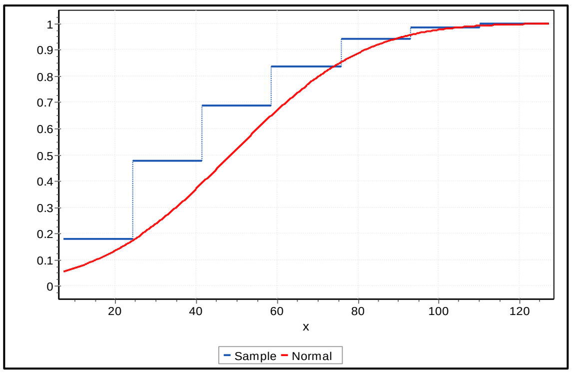

Goodness of Fit Test for Probability Distribution Functions

The easy fit results summary for goodness of fit descriptive and fit statistics for Log Pearson 3, Lognormal, Gumbel Extreme Event and Normal distributions are summarised below;

Table 7: descriptive statistics

Percentile	Value
Min	7.250
5%	11.468
10%	17.302
25% (Q_1)	29.680
50% (Median)	40.040
75% (Q_3)	60.730
90%	88.420
95%	97.890
Max	127.27

Table 10: Percentiles for Annual maximum flows

Statistic	Value
Sample Size, n	67
Range	120.020
Mean	48.725
Variance	671.750
Standard Deviation	25.918
Coefficient of Variation	0.532
Std. Error	3.166
Skewness	0.712
Excess Kurtosis	0.180

Article DOI: https://doi.org/10.37284/eaje.7.1.1670

Table 9: Descriptive statistical parameters

Distribution	Parameters
Gen. Extreme Value	k = -0.03523, s = 21.68, m = 36.943
Log-Pearson 3	a = 8.8531, b = -0.20382, g = 5.5317
Lognormal	s = 0.60191, m = 3.7272
Normal	s = 25.918, m = 48.725

Table 10: Goodness of fit - Anderson-Darling

Distribution	Statistic	Rank
Log-Pearson 3	0.15666	2
Gen. Extreme Value	0.16207	3
Lognormal	0.60765	30
Normal	0.79836	32

Table 11: Goodness of fit for KS

Distribution	Statistic	Rank
Log-Pearson 3	0.04855	13
Gen. Extreme Value	0.05348	18
Lognormal	0.08157	30
Normal	0.10923	38

Gen. – Generalised

Table 12: Goodness of fit test results for Chi squared

Distribution	Statistic	Rank
Log-Pearson 3	0.88502	1
Lognormal	1.4358	6
Gen. Extreme Value	1.7537	14
Normal	0.89	24

From *Table 2* to *Table 12*, quantile magnitudes for the 2, 5 and 10-year return periods are presented. The 2-year quantile estimates are; 44.6 m^3/s, 48.72 m^3/s, 43.59 m^3/s and 51.67 m^3/s for Gumbel, Normal, Log Normal and Log Pearson 3 distributions respectively. These appear to be close to the 50th (second quantile) percentile of 40.042 m^3/s and the mean of 48.73 m^3/s. The 2-year quantile estimates deviates from the 50th percentile and mean by 0.558 m^3/s and 4.13 m^3/s, 6.678 m^3/s and 0.01 m^3/s, 1.548 m^3/s and 5.14 m^3/s, 9.628 m^3/s and 0.94 m^3/s for the Gumbel, Normal, Log Normal and Log Pearson 3 distributions respectively. The 5-year quantile estimates of 67.33 m^3/s, 70.37 m^3/s, 68.92 m^3/s and 63.99 m^3/s for Gumbel, Normal, Log Normal and Log Pearson 3 distributions respectively appear to be closer to the 3rd quantile (75th percentile) of 60.73 m^3/s and deviate from mean. The 5-year quantile estimates deviates from the 75th percentile and mean by 4.6 m^3/s and 18.6 m^3/s, 7.64 m^3/s and 21.64 m^3/s, 6.19 m^3/s and 2019 m^3/s, 1.26 m^3/s and 15.26 m^3/s for the Gumbel, Normal, Log Normal and Log Pearson 3 distributions respectively. The 10-year quantile estimates are; 80.38 m^3/s, 81.69 m^3/s, 87.57 m^3/s and 75.13 m^3/s for Gumbel, Normal, Log Normal and Log Pearson 3 distributions respectively and appear to be close to the 90th percentile of 88.42 m^3/s and deviates from the mean. The 10-year quantile estimates deviates from the 90th percentile and mean by 6.04 m^3/s and 33.65 m^3/s, 6.73 m^3/s and 30.96 m^3/s, 0.85 m^3/s and 36.84 m^3/s, 13.29 m^3/s and 26.4 m^3/s for the Gumbel, Normal, Log Normal and Log Pearson 3 distributions respectively. These results conform with the findings of Ehiorobo and Izinyon (2013b), and Ehiorobo and Uso (2014), during flood frequency analysis at Asejire Dam Site and Oshun river-Nigeria where both Gumbel and Log Pearson Type III distributions produced quantile magnitudes in the same range for the flood

Article DOI: https://doi.org/10.37284/eaje.7.1.1670

frequency analysis for 25 years and below return periods. Therefore, for specified return periods, Gumbel and LP III provide similar quantile estimates and can be utilized for flood frequency analysis at 25 years and below return periods.

Similaly, it is observed that both Gumbel and Log Pearson 3 distributions generate extreme magnitudes of discharge close to maximum quantitle of 127.27 m^3/s. The 100-year and 200-year return period quantitle estimates are 129.51 m^3/s and 126.93 m^3/s, and 143.46 m^3/s and 148.29 m^3/s for Gumbel and Log Pearson 3 respectively. These deviate from the maximum quantile by 0.24 m^3/s and 0.34 m^3/s, and 16.19 m^3/s and 21.02 m^3/s for the Gumbel and Log Pearson 3 respectively. According to Ehiorobo and Izinyon (2013b), different probability distributions have generated related results for small to medium sized return periods but also produce very different estimates for larger events.

Log Normal distribution (LN) presents the highest quantile estimate for 200-yr return period at 177.16 m^3/s followed by the Log Pearson 3 distribution at 148.29 m^3/s and the lowest quantile estimate for the 2-year return period at 43.59 m^3/s and 51.67 m^3/s respectively. Previous studies by Kundu et al. (2014), to evaluate the effects of climate change on flood frequency in Luvuvhu river catchment in South Africa revealed that LN and LP 3 exhibited the highest and similar probability densities with higher frequencies than that of GEV and EVI distributions. A similar study by Ibrahim et al. (2016), to determine the flood frequency analysis at Hadejia River in Nigeria revealed that Log Normal distribution predicted highest quantile values as compared to Log Pearson 3 and Gumbel distributions.

An experiment at Oshun river site, Log Normal distribution predicted higher values and was recommended for use for flood frequency analysis in that location as it creates favourable conditions for higher discharge at higher recurrence interval (Ehiorobo & Uso, 2014).

From Table 4.6 and Figure 4.6, there is an increasing upward trend of discharges at Manafwa River at higher probabilities of exceedance across all the probability distributions. This agrees with; Bai et al. (2019), Kundu et al. (2014), Sinshaw et al. (2018) and Bhat et al. (2019) who observed that increasing magnitudes of extreme hydrological discharges are due to varrying climatic changes and rapid landuse changes in the catchment.

To establish the best distribution parameter that best suits the discharge data and generates best output, the data available was used to draw graphs and the most fit regression coefficient obtained. These results are in agreement with the findings of Malik and Pal (2021), where Log Pearson Type 3 shows flood values being higher in lower Dwarkeswar River, Eastern India.

Figure 12: Annual maximum flows vs. exceedance probability

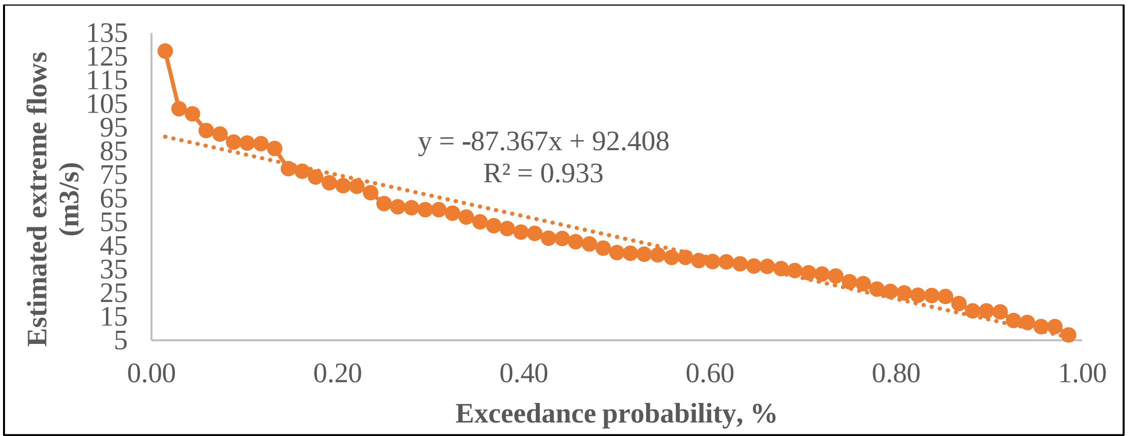

Article DOI: https://doi.org/10.37284/eaje.7.1.1670

Figure 13: Annual maximum flows vs. reduced y-variate

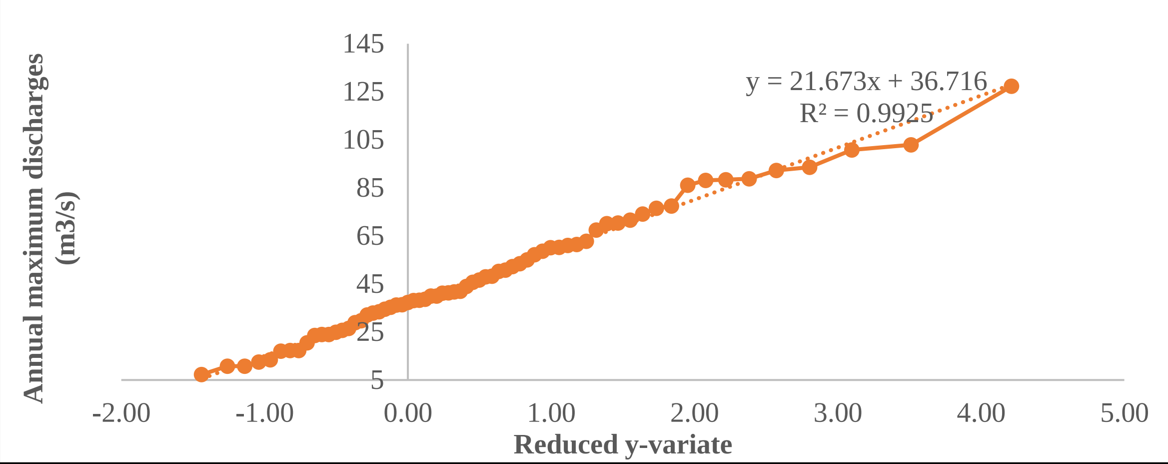

Figure 14: Extreme discharges of different probability functions vs. return periods

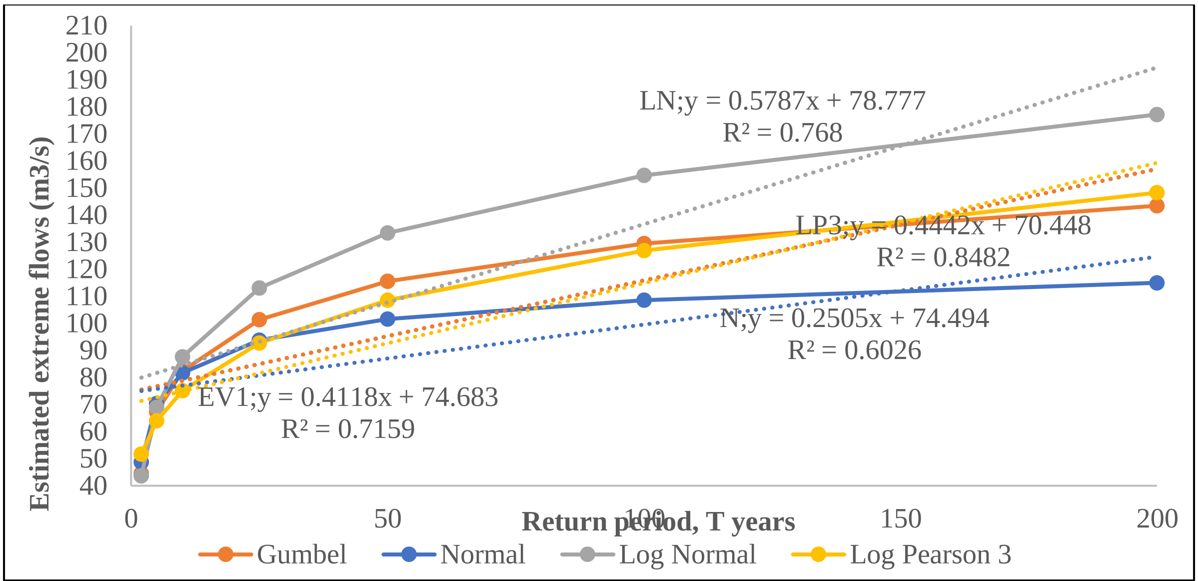

Table 13: Regression coefficients and line equations

Probability distribution functions	Equation of the line, y =	Regression coefficient, R^2
Gumbel	0.4118x+74.683	0.7159
Normal	0.2505x+74.494	0.6026
Log Normal	0.5758x+78.77	0.768
Log Pearson 3	0.4442x+70.448	0.8482

From *Figure 13* to *Figure 14*, and *Table 13* for the goodness of fit plot to determine the linearity of probability, both Log Normal and Log Pearson 3 distributions have more linear plots than the rest. It should also be noted that Log Pearson 3 that has the skew coefficient also includes log-normal whose skew value of the logarithms is zero (Roy et al., 2015). From Table 4.13, the regression line for the Log Pearson 3 probability distribution presents the most accurate regression coefficient at 0.8482 and suits best the available data.

The goodness of fit test results for the Anderson-Darling test show that the Log Pearson 3 produced the best result followed by the Generalised Extreme Value (GEV1) with statistics of 0.15666 and 0.16207 respectively. Similarly, the Kolmogorov-Smirnov test show that among four probability distributions under study (Log Pearson 3, Gumbel/EV1, Lognormal and normal),

Article DOI: https://doi.org/10.37284/eaje.7.1.1670

the Log Pearson 3 produced the best result followed by the Generalised Extreme Value (GEV1) with statistics of 0.04855 and 0.05348 respectively. These results satisfy findings of Singo et al. (2016), during a study to evaluate flood risks of Luvuvhu River Catchment in South Africa using flood frequency models; concluded that the Gumbel and Log-Pearson Type 3 distributions models provide the best fit and are usually chosen to undertake the flood frequency analysis. These results support the findings by Pamuttu et al. (2018). In his study to select distribution method for rainfall in Bengawan watershed he found the Log Pearson 3 to be the best distribution based on the Smirnov-Kolmogorov test. The findings of this study are also supported by Farooq et al. (2018) who in his study to analyse floods and best fit using LP 3, LN, GEV and normal distributions methods found Log Pearson 3 distribution ranked top followed by GEV1.

Goodness of Fit Test For Normality

Chi squared test for goodness of fit is as per the table below;

Table 14: Chi squared test goodness of fit table

Range	Freq	f(x)	Cum Freq, F(x)	z	z-values	$F(x_i)$	p(x)	χ^2
0-10	1.0	0.015	0.015	-1.505	0.933	0.067	0.067	0.699
10-20	7.0	0.104	0.119	-1.117	0.867	0.134	0.067	1.434
20-30	9.0	0.134	0.254	-0.728	0.767	0.233	0.099	0.833
30-40	13.0	0.194	0.448	-0.339	0.633	0.367	0.134	1.787
40-50	9.0	0.134	0.582	0.050	0.516	0.516	0.149	0.098
50-60	7.0	0.104	0.687	0.438	0.670	0.670	0.154	1.067
60-70	6.0	0.090	0.776	0.827	0.797	0.797	0.127	0.730
70-80	6.0	0.090	0.866	1.216	0.889	0.889	0.092	0.005
80-90	4.0	0.060	0.925	1.605	0.945	0.945	0.056	0.013
90-100	0.0	0.030	0.955	1.993	0.977	0.977	0.032	0.006
100-110	0.0	0.030	0.985	0.382	0.991	0.991	0.015	1.067
110-120	0.0	0.000	0.985	0.771	0.997	0.997	0.006	0.395
120-130	1.0	0.015	1.000	3.160	0.999	0.999	0.002	5.597
n		67					$\sum\chi^2$	15.731
Mean, μ		48.7					df	10.000
Std dev, σ		25.7					$\chi^2_{0.05,10\ df}$	18.310
				Calculated $\chi^2 <$ tabular χ^2				Accept

Std dev – standard deviation, Cum freq - Cumulative Frequency, Freq - Frequency

Figure 15: Histogram of freq vs intervals

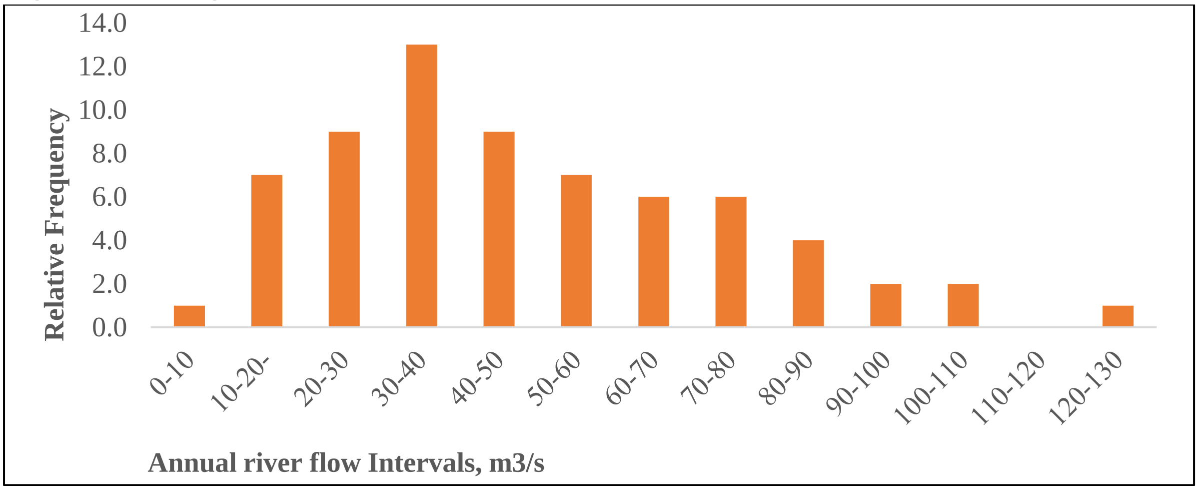

Article DOI: https://doi.org/10.37284/eaje.7.1.1670

Figure 16: Cum freq vs annual maximum flows

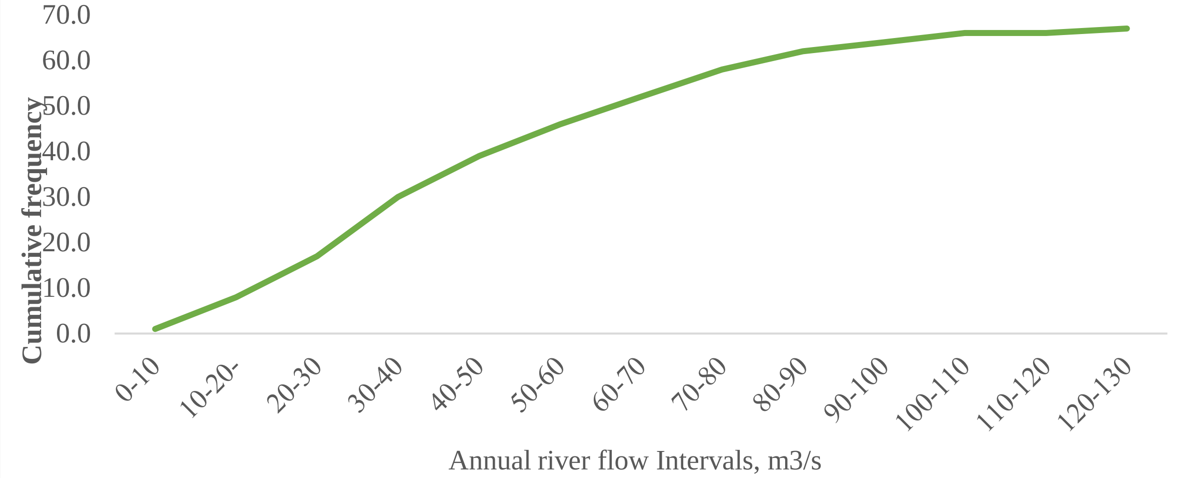

K-S test for goodness of fit is as below;

Table 15: Kolmogorov-Smirnov, K-S test goodness of fit table

Range	Frequency	Cum freq	$F_s(x)$	z	z-values	$F(x_i)$	D_n
0-10	1	1.0	0.015	-1.505	0.933	0.067	0.052
10-20	7	8.0	0.119	-1.117	0.867	0.134	0.014
20-30	9	17.0	0.254	-0.728	0.767	0.233	-0.021
30-40	13	30.0	0.448	-0.339	0.633	0.367	-0.081
40-50	9	39.0	0.582	0.050	0.516	0.516	-0.066
50-60	7	46.0	0.687	0.438	0.670	0.670	-0.017
60-70	6	50.0	0.776	0.827	0.797	0.797	0.021
70-80	6	58.0	0.866	1.216	0.889	0.889	0.023
80-90	4	60.0	0.925	1.605	0.945	0.945	0.020
90-100	2	64.0	0.955	1.993	0.977	0.977	0.021
100-110	2	66.0	0.985	0.382	0.991	0.991	0.006
110-120	0	66.0	0.985	0.771	0.997	0.997	0.012
120-130	1	67.0	1.000	3.160	0.999	0.999	-0.001
n	67						

From Equation 30, $D_{critical}$ is 0.166 and from Table 15, D_n is 0.05 A comparison between $D_{critical}$ and D_n shows that D_n (0.052) < $D_{critical}$ (0.166) implying there is no significant relationship between the treatments. The goodness of fit tests by Chi-square test shows that normal distribution best fits the data with calculated χ^2< tabular χ^2 (15.731 < 18.31). The K-S test for the goodness of fit also shows that there is no significant relationship between the treatments. This is supported by Suhartanto et al. (2018), during the study to estimate design flood with four frequency analysis of the Lesti-sub-catchment in Indonesia whose results indicate that LP3 is accepted for two testing of goodness of fit and has minimum deviation. The result is supported by Manta and Ahaneku (2009), during flood frequency analysis of Gurara River catchment in Nigeria that found Log Pearson 3 distribution as the best data fit. Results of the Log Pearson 3 distribution as the most accurate and best fit model are further supported by Olofintoye et al. (2009), during the study to determine best–fit probability distribution model for peak daily rainfall of selected cities in Nigeria which observed Log Pearson 3 distribution as the best to fit peak precipitation. These results support the findings by Pamuttu et al. (2018) who observed that Gumbel Distribution and Log Pearson III were the best distribution based on Chi square test since they produce Chi-Square value < Chi Critical.

Article DOI: https://doi.org/10.37284/eaje.7.1.1670

CONCLUSION AND RECOMMENDATIONS

From the results, it is observable that the 2-year quantile estimates are; 44.6 m^3/s, 48.72 m^3/s, 43.59 m^3/s and 51.67 m^3/s for Gumbel, Normal, Log Normal and Log Pearson 3 distributions respectively. The 5-year quantile estimates are; 67.33 m^3/s, 70.37 m^3/s, 68.92 m^3/s and 63.99 m^3/s for Gumbel, Normal, Log Normal and Log Pearson 3 distributions respectively. The 10-year quantile estimates are; 80.38 m^3/s, 81.69 m^3/s, 87.57 m^3/s and 75.13 m^3/s for Gumbel, Normal, Log Normal and Log Pearson 3 distributions respectively. Similaly, it is observed that both Gumbel and Log Pearson 3 distributions generate extreme magnitudes of discharge close to maximum quantitle of 127.27 m^3/s. The 100-year and 200-year return periods quantitle estimates are 129.51 m^3/s and 126.93 m^3/s, and 143.46 m^3/s and 148.29 m^3/s for Gumbel and Log Pearson 3 respectively. From the study above, there is an increasing upward trend of the extreme discharges at Manafwa River floodplains at higher probabilities of exceedance across all the probability distributions due to the varrying climatic changes and rapid land-use changes in the catchment. The goodness of fit plot to determine the linearity of the probability showed that both Log Normal and Log Pearson 3 distributions have more linear plots than GEV and EVI. The regression line for the Log Pearson 3 probability distribution presents the most accurate regression coefficient at 0.8486 as compared to the others.

REFERENCES

Agrawal, S., Gopalakrishnan, T., Gorokhovich, Y., & Doocy, S. (2013). Risk factors for injuries in landslide- and flood-affected populations in Uganda. Prehospital and Disaster Medicine, 28(4), 314–321. https://doi.org/10.1017/S1049023X13000356

Alghazali, N. O., & Alawadi, D. A. (2014). Fitting statistical distributions of monthly rainfall for some Iraqi stations. Civil and Environmental Research, 6(6), 40–46.

Aslam, M. (2019). Introducing Kolmogorov–Smirnov tests under uncertainty: an application to radioactive data. ACS Omega, 5(1), 914–917.

Bai, Y., Zhang, Z., & Zhao, W. (2019). Assessing the impact of climate change on flood events using HEC-HMS and CMIP5. Water, Air, & Soil Pollution, 230(6), 1–13.

Bhat, M. S., Alam, A., Ahmad, B., Kotlia, B. S., Farooq, H., Taloor, A. K., & Ahmad, S. (2019). Flood frequency analysis of river Jhelum in Kashmir basin. Quaternary International, 507, 288–294. https://doi.org/10.1016/j.quaint.2018.09.039

Bingwa, F. (2013). A quantitative analysis of the impact of land use changes on floods in the Manafwa River Basin. Massachusetts Institute of Technology.

Cecinati, F. (2013). Precipitation analysis for a flood early warning system in the Manafwa River Basin, Uganda. Massachusetts Institute of Technology.

Châu, V. N. (2014). Assessing the Impacts of Extreme Floods on Agriculture in Vietnam : Quang Nam Case Study. 214.

Chow, V. Te, Maidment, D. R., & Mays, L. W. (1988). Applied_Hydrology_Chow_1988. McGraw-Hill.

Dis, M. O., Anagnostou, E., & Mei, Y. (2018). Using high-resolution satellite precipitation for flood frequency analysis: case study over the Connecticut River Basin. Journal of Flood Risk Management, 11, S514–S526. https://doi.org/10.1111/jfr3.12250

Ehiorobo, J. O., & Izinyon, O. C. (2013b). Flood Frequency Analysis at Oshun River in Asejire Dam Site, Nigeria. In Journal of Earth Science and Engineering (Vol. 3).

Ehiorobo, J. O., & Uso, N. O. (2014). Flood Frequency Analysis in the Lower River Niger Basin at Onitsha. Journal of Engineering Research, 19(1). www.waado.org/nigerdelta/

nigeria_facts/nigerianmaps/nigeria_cities.html

Farooq, M., Shafique, M., & Khattak, M. S. (2018). Flood frequency analysis of river swat using Log Pearson type 3, Generalized Extreme Value, Normal, and Gumbel Max distribution methods. Arabian Journal of Geosciences, 11(9). https://doi.org/10.1007/s12517-018-3553-z

Franks, S. W., & Kuczera, G. (2002). Flood frequency analysis: Evidence and implications of secular climate variability, New South Wales. Water Resources Research, 38(5), 20-1-20–27. https://doi.org/10.1029/2001wr000232

Ibrahim, U. A., Yadima, S. G., & Nur Alkali, A. (2016). Flood Frequency Analysis at Hadejia River in Hadejia–Jama'are River Basin, Nigeria. Civil and Engineering Research, 8(9), 514–2225.

Kamal, V., Mukherjee, S., Singh, P., Sen, R., Vishwakarma, C. A., Sajadi, P., Asthana, H., & Rena, V. (2017a). Flood frequency analysis of Ganga river at Haridwar and Garhmukteshwar. Applied Water Science, 7(4), 1979–1986.

Kundu, P. M., Singo, R. L., Odiyo, J. O., & Nkuna, R. N. (2014). An evaluation of the effects of climate change on flood frequency in the luvuvhu river catchment, limpopo province, south africa. WIT Transactions on Ecology and the Environment, 185, 157–168. https://doi.org/10.2495/SI140151

Malik, S., & Pal, S. C. (2021). Potential flood frequency analysis and susceptibility mapping using CMIP5 of MIROC5 and HEC-RAS model: a case study of lower Dwarkeswar River, Eastern India. SN Applied Sciences, 3(1). https://doi.org/10.1007/s42452-020-04104-z

Manta, H., & Ahaneku, E. (2009). Flood frequency analysis of Gurara River catchment at Jere, Kaduna State, Nigeria. Scientific Research and Essay, 4(6), 636–646. http://www.academicjournals.org/SRE

Masood, M., & Takeuchi, K. (2012). Assessment of flood hazard, vulnerability and risk of mid-eastern Dhaka using DEM and 1D hydrodynamic model. Natural Hazards, 61(2), 757–770.

Mayega, R. W., Tumuhamye, N., Atuyambe, L., Okello, D., Bua, G., Ssentongo, J., & Bazeyo, W. (2015). Qualitative assessment of resilience to the effects of climate variability in the three communities in Uganda. In RAN Secretariat and East African Resilience Innovation Lab (EA RILab), Kampala.

Mehmood, A., Jia, S., Mahmood, R., Yan, J., & Ahsan, M. (2019). Non-stationary Bayesian modeling of annual maximum floods in a changing environment and implications for flood management in the Kabul River Basin, Pakistan. Water, 11(6), 1246.

Njoku, C., Njoku, C., & Okoro, G. C. (2015). Effect of flooding on soil properties in Abakaliki South-Eastern Nigeria Physico-chemical analysis of water from some selected automobile repairing area in Abakaliki Southeastern Nigeria View project Soil Properties View project Effect of flooding on soil. Scholarly Journal of Agricultural Science, 5(5), 165–168. https://doi.org/10.13140/RG.13314.12489

Njoku, C., & Okoro, G. C. (2015). Effect of flooding on soil properties in Abakaliki South-Eastern Nigeria. Scholarly Journal of Agricultural Science, 5(5), 165–168. http://www.scholarly-journals.com/SJAS

Obubu, J. P., Mengistou, S., Fetahi, T., Alamirew, T., Odong, R., & Ekwacu, S. (2021). Recent climate change in the lake kyoga basin, Uganda: An analysis using short-term and long-term data with standardized precipitation and anomaly indexes. Climate, 9(12). https://doi.org/10.3390/cli9120179

Odunuga, S., & Raji, S. A. (2014). Flood Frequency Analysis and Inundation Mapping

Article DOI: https://doi.org/10.37284/eaje.7.1.1670

of Lower Ogun River Basin. In Journal of Water Resource and Hydraulic Engineering Sept (Vol. 3, Issue 3).

Ogbodo, E. N. (2011). Assessment of Some Soil Fertility Characteristics of Abakaliki Urban Flood Plains of South-East Nigeria, for Sustainable Crop Production. World Journal of Agricultural Sciences, 7(4), 489–495.

Ogwang, B. A., Guirong, T., & Haishan, C. (2012). (droughts) experienced in the years. In Pakistan Journal of Meteorology (Vol. 9).

Olofintoye, O. O., Sule, B. F., & Salami, A. W. (2009). Best–fit Probability distribution model for peak daily rainfall of selected Cities in Nigeria. New York Science Journal, 2(3), 1–1

Pamuttu, D. L., Lasminto, U., Pasalli, D. A., Rada, Y. H. M., & Doloksaribu, A. (2018). The Selection of Rain Distribution Analysis Method in (Bengawan Solo Watershed) Downstream Sub-Watershed. International Conference on Science and Technology (ICST 2018), 416–420.

Roy, P. K., Roy, P., & Kumar De, S. (2015). A comparative approach to flood frequency analysis of the Puthimari river in Assam, India. In asian journal of spatial science (vol. 3).

Singo, L. R., Kundu, P. M., Mathivha, F. I., & Odiyo, J. O. (2016). Evaluation of flood risks using flood frequency models: a case study of Luvuvhu River Catchment in Limpopo Province, South Africa. Urban Water III, 1, 215–226. https://doi.org/10.2495/uw160191

Sinshaw, B. G., Moges, M. A., Kinde Tefera, A., Birhan Atanaw, S., Fenta, H. M., Bazezew, H. A., Geletaw Eshete, D., & Legese, K. G. (2018). Analysis of regional flood frequency and its socio-economic impact in Ethiopia. 12(12). https://doi.org/10.5897/AJEST2018.xxxx

Suhartanto, E., Montarcih Limantara, L., Noviadriana, D., Iman Harta, F., & Aryani, D. K. (2018). Estimation of Design Flood with Four Frequency Analysis Distributions. In Asian Journal of Applied Science and Technology (AJAST) (Open Access Quarterly International Journal (Vol. 2, Issue 1). www.ajast.net

Thomopoulos, N. T., Thomopoulos, N. T., & Philipson. (2018). Probability Distributions. Springer.

Wan Deraman, W. H. A., Abd Mutalib, N. J., & Mukhtar, N. Z. (2017). Determination of return period for flood frequency analysis using normal and related distributions. Journal of Physics: Conference Series, 890(1). https://doi.org/10.1088/1742-6596/890/1/012162